

Establishment of AC Power Standard at Frequencies Up to 100 kHz

Zhaomin Shi¹, Jiangtao Zhang², Xianlin Pan², Qing He², Jun Lin¹

¹*College of Instrumentation and Electrical Engineering, Jilin University, Changchun, China, shizhaominnim@163.com, 86 10 64526541*

²*National Institute of Metrology, Beijing, China, zhangjt@nim.ac.cn, 86 10 64524514*

Abstract – This paper describes the establishment of wideband power standard for traceable measurements of electrical power of sinusoidal signals. The voltage ranges from 10 V to 600 V and the current ranges from 1 A to 100 A at frequencies up to 100 kHz. The design of the power system and the components, including resistive voltage dividers (RVDs), current shunts and dual-channel digitizer have been presented. The amplitude errors of RVDs and shunts are calibrated and traceable to the dc standard based on the ac-dc transfer technique. The self-calibration of RVDs and current shunts in phase angle errors has also been described respectively. The phase angle between two channels of the digitizer has been calibrated. The measurement results of each component have been given both in the amplitude and phase angle errors. The final uncertainty of the power standard for 100 V and 100 A has been given at frequencies ranging from 400 Hz to 100 kHz.

Keywords – Power measurement, resistive voltage divider, current shunt, phase angle errors, dual-channel digitizer

I. INTRODUCTION

With the development in the fields of smart grid, energy conservation and emission reduction, requirement for the wideband power measurement with high precision has been put forward. In recent years many commercially instrumentation for wideband power analysis, voltage and current measurement, and other fields like this have appeared. This generates a need to establish power standard to provide traceability for these instruments.

Several national metrology institutes are working on establishment of national power standard. A fully traceable standard of electrical power at frequencies up to 200 kHz has been established at the National Measurement Institute, Australia (NMIA) [1]. The standard establishment is based on thermal power comparator (TPC) [2]. The power standard for frequencies up to 1 MHz is reported in [3] by RISE Research Institutes of Sweden. The voltage ranges up to

20 V at 1 MHz and current up to 100 A at 100 kHz, and 1 A at 1 MHz.

At the National Institute of Metrology (NIM), China, national power standard has been established at frequencies up to 100 kHz and can provide traceability for the commercially instruments. A set of RVDs with serial-parallel connection has been designed and self-calibrated. The cage-like current shunts have been built and calibrated against a time constant standard. A dual-channel digitizer is used to measure the phase angle errors between two voltage signals.

II. MEASUREMENT SYSTEM

The power measurement system is shown in Fig. 1. It includes the power generator part and measurement part. The phase standard, Clark-Hess CH 5500-2, is used as the dual-channel ac voltage source to produce two voltage signals with arbitrary degrees and amplitudes. The power amplifier, Fluke 5205A, is to extend the voltage ranges. Clarke-Hess CH 8100 is used as the transconductance amplifier to make the current reach 100 A at 100 kHz. The power analyzer is the device under test (DUT).

The measurement part of the system includes a set of RVDs and current shunts for different voltage and current ranges respectively. RVDs and current shunts are used to convert the high voltage and current signals of power to the two voltage signals which can be measured by the sampling system. The phase angle between the two voltage signals, marked as U_1 and U_2 in Fig. 1, can be measured by the dual-channel digitizer from National Instruments, NI-PXI-5922. The amplitudes of the two voltage signals can also be measured against two AC voltmeters, Fluke 5790A. The measurement system connects with a computer by IEEE-488 bus.

III. RESISTIVE VOLTAGE DIVIDERS

Due to the wide band and good linearity, we choose to use RVDs as the voltage dividers in the system. A set of RVDs with serial-parallel connection has been designed at NIM [4]. The structure of the RVD is shown in Fig. 2. The upper part of the RVD contains m sets of resistors in

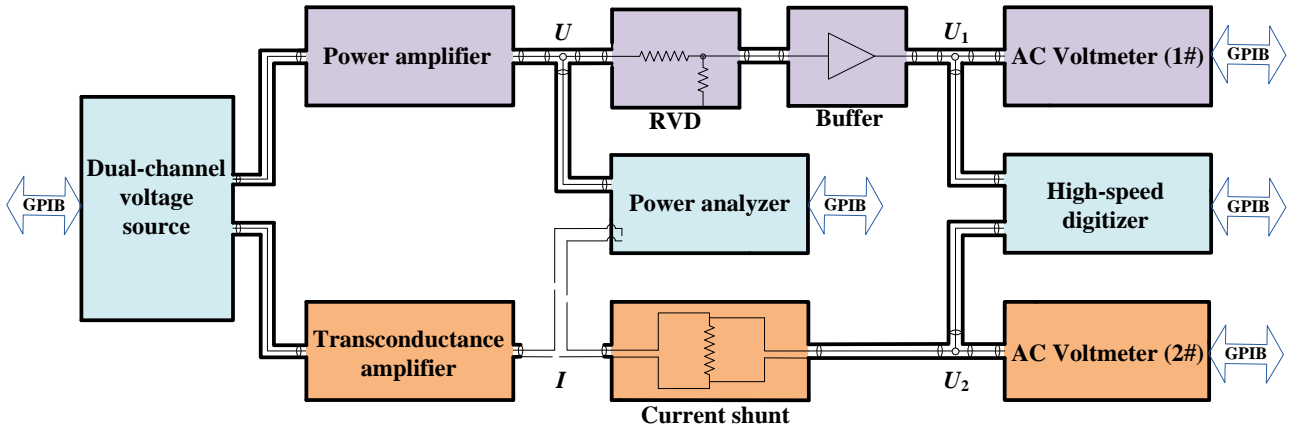


Fig. 1. Diagram of national power standard system

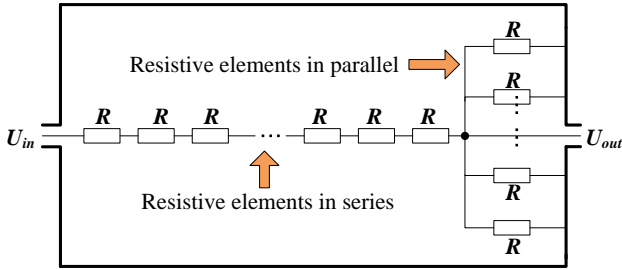


Fig. 2. Basic structure of RVD with serial-parallel connection

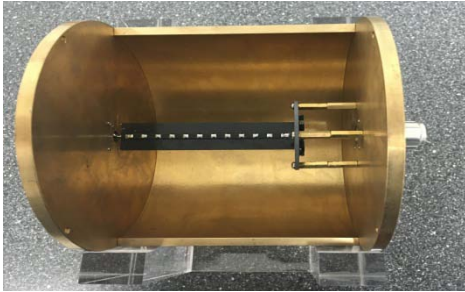


Fig. 3. RVD with ratio of 100:1

serial connection and the lower part contains n sets of resistors in parallel connection. The resistive elements used are thin-film resistors from Vishay Company with high stability and all the resistors in one RVD have been chosen to be identical. To meet the requirements of the voltages from 10 V up to 600 V, RVDs with different ratios and different resistances have been built. Fig. 3 shows the physical map of 100:1 RVD. This RVD is built with 11 sets of 100 Ω resistors in serial connection and 9 sets of 100 Ω resistors in parallel. A buffer amplifier is introduced to reduce the external loading errors of the RVDs in the practical application.

The amplitude errors of the RVDs can be calibrated and traceable to the dc voltage standard by ac-dc conversion with thermal voltage converters (TVCs). The amplitude errors of RVDs with different ratios are shown in Fig. 4. As seen from the figure, the amplitude errors of

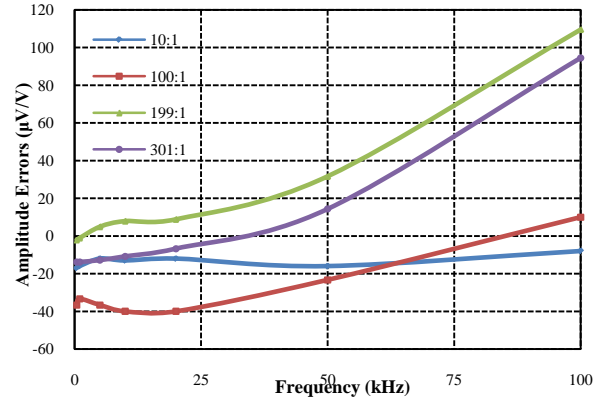


Fig. 4. Amplitude errors of RVDs with different ratios

the RVDs are less than 120 $\mu\text{V/V}$ at 100 kHz.

For the RVD with serial-parallel connection, the phase angle errors are mainly caused from the capacitive leakage influence, including the leakage capacitance from resistive elements to the housing of RVD, and the capacitance across each resistor in the RVD. The phase angle error from the leakage capacitance can be expressed as

$$\theta = - \left\{ \left(\sum_{i=1}^m \frac{(i \times n \times (m-i) + i)}{mn+1} \times C_i + \frac{m}{mn+1} \times C_p \right) - \left(\sum_{x=0}^{m-1} \sum_{i=x+1}^m \frac{(i-x)^2 \times n}{mn+1} \times C_{xi} \right) \right\} \times \omega R \quad (1)$$

$$= -f(C) \times \omega R$$

where C_i is the equivalent leakage capacitance between each resistive element in series part and the shell of RVD, C_p is the equivalent capacitance between the resistive elements in parallel part and the shell, C_{xi} is the capacitive leakage across each resistor, m is the number of resistors in serial connection, n is the number of resistors in parallel, ω is angle frequency, and R is the

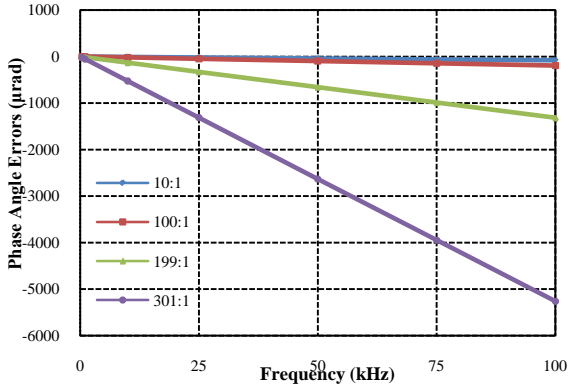


Fig. 5. Phase angle errors of RVDs with different ratios

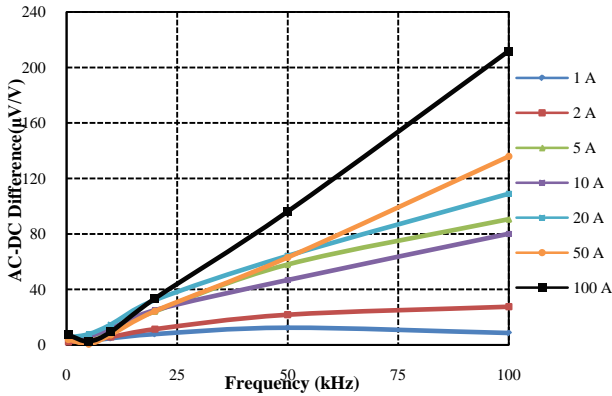


Fig. 6. AC-DC difference of shunts with different rated currents

resistance of each resistive element. According to (1), the phase angle error is in proportional relationship with the leakage capacitance and resistance at the same frequency. The leakage capacitance is determined by the structure parameter, and can be seen equal in the RVDs with identical physical structure. So a new method is proposed to calibrate the phase angle errors. Two RVDs with identical structure but different resistances have been built and the phase angle difference between the two RVDs is measured, then the absolute phase error of one RVD can be derived from the phase difference. The phase angle errors of RVDs with different ratios have been calibrated and the results are shown in Fig. 5. The calibration results show well frequency response at frequency range from 400 Hz to 100 kHz.

IV. CURRENT SHUNTS

A set of current shunts with cage-like design using high-precision thin-film resistors has been built and used in the power system. The traceability of the ratio errors of current shunts can be realized by determining the dc resistance and ac-dc difference. The ac-dc difference of the shunts with different rated currents is measured with thermoelectric effects and shown in Fig. 6.

A 1-Ω shunt of coaxial design has been developed as the time constant standard at NIM [5] and the basic

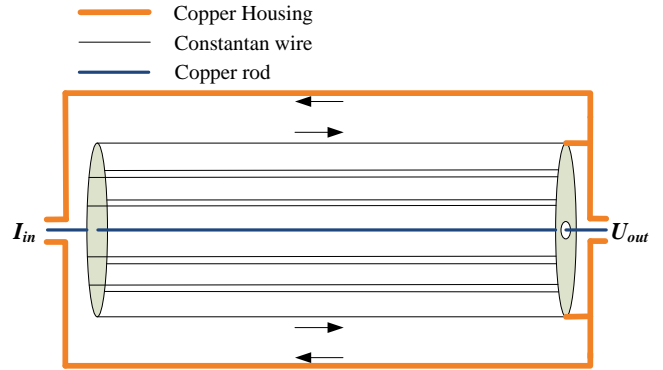


Fig. 7. Basic structure of time constant standard

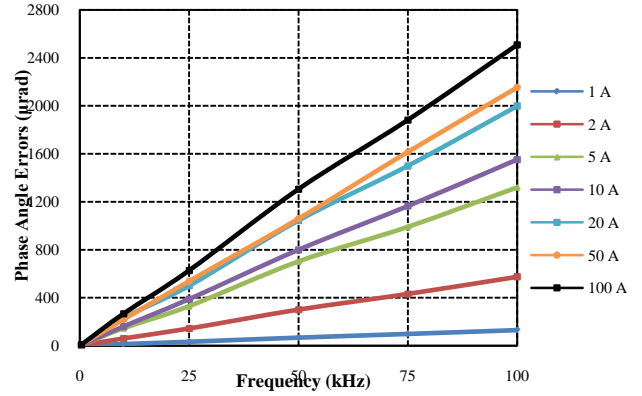


Fig. 8. Phase angle errors of shunts with different rated currents

structure is shown in Fig. 7. The coaxial shunt contains eighteen constantan wires with a diameter of 0.6 mm and length of 105 mm in parallel connection. These constantan wires evenly distribute along a circular surface between two printed circuit boards with copper layer. The current input terminal is connected to the core of the copper board and current is fed through the constantan wires to the copper housing of shunt as current loop. For voltage loop, the copper rod is connected to the core of the same copper board as the voltage high terminal and the housing is the low terminal. The time constant is determined by calibrating the resistance, distributed capacitance and inductance of the shunt respectively.

The phase angle errors of current shunts can be calibrated against the time standard. For high current shunts, the phase angle errors can be measured against a phase angle reference standard with only one step [6], based on the use of a three-branch binary inductive current divider. A low current cage-like shunt combined with a 100:1 IVD is used as the phase angle reference standard. The phase angle error of the low current shunt can be measured against the time standard. The IVD is calibrated with a RVD which can be self-calibrated. The loading error can be also determined. Then the phase angle reference standard are finally calibrated and used to measure the phase angle errors of high current shunts.

Table 1. Uncertainty budget of ac power standard for 100 V and 100 A at frequencies from 400 Hz to 100 kHz.

Component	Unit	Power factor	0.4	1	10	20	50	100
Ratio influence of RVD with buffer	$\mu\text{V}/\text{V}$	1	21.0	30.0	35.0	40.0	45.0	60.0
		0.5	10.5	15.0	17.5	20.0	22.5	30.0
		0	0.0	0.0	0.0	0.0	0.0	0.0
Phase influence of RVD with buffer	μrad	1	0.0	0.0	0.0	0.0	0.0	0.0
		0.5	4.3	6.1	13.0	17.3	24.2	39.0
		0	5.0	7.0	15.0	20.0	28.0	45.0
DC resistance of shunt	$\mu\Omega/\Omega$	1	5.0	5.0	5.0	5.0	5.0	5.0
		0.5	2.5	2.5	2.5	2.5	2.5	2.5
		0	0.0	0.0	0.0	0.0	0.0	0.0
Shunt AC-DC difference	$\mu\Omega/\Omega$	1	20.0	25.0	32.0	40.0	50.0	65.0
		0.5	10.0	12.5	16.0	20.0	25.0	32.5
		0	0.0	0.0	0.0	0.0	0.0	0.0
Shunt phase error	μrad	1	0.0	0.0	0.0	0.0	0.0	0.0
		0.5	10.4	13.9	17.3	23.4	34.6	47.6
		0	12.0	16.0	20.0	27.0	40.0	55.0
Digitizer phase error	μrad	1	0.0	0.0	0.0	0.0	0.0	0.0
		0.5	2.6	3.5	4.3	6.1	8.7	13.0
		0	3.0	4.0	5.0	7.0	10.0	15.0
AC voltmeter(1#) error	$\mu\text{V}/\text{V}$	1	4.0	5.0	7.0	10.0	15.0	20.0
		0.5	2.0	2.5	3.5	5.0	7.5	10.0
		0	0.0	0.0	0.0	0.0	0.0	0.0
AC voltmeter(2#) error	$\mu\text{V}/\text{V}$	1	4.0	5.0	7.0	10.0	15.0	20.0
		0.5	2.0	2.5	3.5	5.0	7.5	10.0
		0	0.0	0.0	0.0	0.0	0.0	0.0
External loading effect of buffer on ratio	$\mu\text{V}/\text{V}$	1	0.5	0.5	1.0	2.0	4.0	16.0
		0.5	0.3	0.3	0.5	1.0	2.0	8.0
		0	0.0	0.0	0.0	0.0	0.0	0.0
External loading effect of buffer on phase angle	μrad	1	0.0	0.0	0.0	0.0	0.0	0.0
		0.5	0.4	0.4	0.9	1.7	3.5	6.9
		0	0.5	0.5	1.0	2.0	4.0	8.0
Shunt loading effect on ratio error	$\mu\text{V}/\text{V}$	1	0.5	0.5	0.5	1.0	1.0	2.0
		0.5	0.3	0.3	0.3	0.5	0.5	1.0
		0	0.0	0.0	0.0	0.0	0.0	0.0
Shunt loading effect on phase angle error	μrad	1	0.0	0.0	0.0	0.0	0.0	0.0
		0.5	0.4	0.4	0.4	0.9	1.3	1.7
		0	0.5	0.5	0.5	1.0	1.5	2.0
Common mode interference on ratio	$\mu\text{V}/\text{V}$	1	5.0	5.0	10.0	15.0	18.0	23.0
		0.5	2.5	2.5	5.0	7.5	9.0	11.5
		0	0.0	0.0	0.0	0.0	0.0	0.0
Common mode interference on phase angle	μrad	1	0.0	0.0	0.0	0.0	0.0	0.0
		0.5	4.3	4.3	8.7	13.0	15.6	17.3
		0	5.0	5.0	10.0	15.0	18.0	20.0
Reactive coupling influence on ratio	$\mu\text{V}/\text{V}$	1	2.0	2.0	5.0	6.0	8.0	12.0
		0.5	1.0	1.0	2.5	3.0	4.0	6.0
		0	0.0	0.0	0.0	0.0	0.0	0.0
Reactive coupling influence on phase angle	μrad	1	0.0	0.0	0.0	0.0	0.0	0.0
		0.5	3.5	4.3	6.9	8.7	10.4	13.0
		0	4.0	5.0	8.0	10.0	12.0	15.0
Combined uncertainty	$\mu\text{W}/\text{VA}$	1	31	41	50	61	74	98
		0.5	20	27	36	46	60	83
		0	15	20	29	39	55	78
Expanded uncertainty	$\mu\text{W}/\text{VA}$	1	62	82	100	122	148	196
		0.5	40	54	72	92	120	166
		0	30	40	58	78	110	156

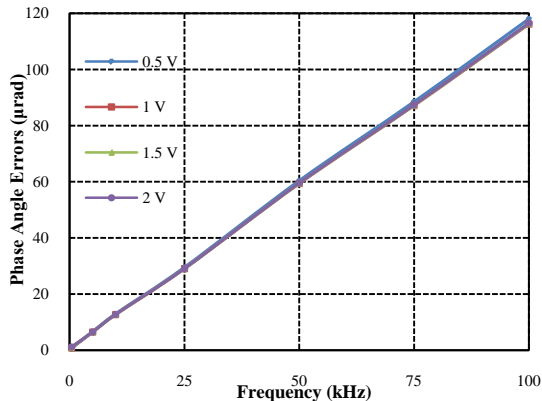


Fig. 9. Phase angle errors of dual-channel digitizer

The level dependence in phase angle errors of high current shunts has also been evaluated. The phase angle errors of resistive shunts with different rated currents are shown in Fig. 8.

V. CALIBRATION OF DUAL-CHANNEL DIGITIZER

The phase angle errors between two voltage signals can be measured by the dual-channel digitizer, NI-PXI-5922. But there is phase angle existing between the two channels of the digitizer and need to be calibrated. Phase error of the digitizer has been measured at different phase angles between the channels in [7]. The results appeared not depend on the phase angles. In addition, the phase error may change at different input voltages and the linearity error has been taken into account. The phase angle error can be determined by connecting the two channels with the same source and measured at different input voltages. The sampling frequency is determined by input voltage frequency. For input voltage at frequencies up to 100 kHz, the sampling frequency is set to be 10 MHz. The final results are the average of multiple measurement results and shown in Fig. 9 at voltage range from 0.5 V to 2 V. The phase error between two channels is within 120 μrad at 100 kHz and the linearity error at different voltages is less than 10 μrad .

VI. UNCERTAINTY ANALYSIS

The uncertainty of ac power standard for different voltages and currents has been analyzed. The uncertainty budget for 100 V and 100 A at different power factors is

shown in Table I. The frequency ranges from 400 Hz to 100 kHz. The uncertainty of power standard is less than 100 $\mu\text{W}/\text{VA}$ for 100 V and 100 A at 100 kHz at power factor 1. At power factor 1, the dominant components are from the RVD ratio uncertainty and ac-dc difference of current shunt, whereas at power factor 0, the uncertainty is dominated by the phase uncertainty of RVD and shunt.

VII. CONCLUSION

The national power standard has been developed at frequencies up to 100 kHz and provides traceability for the power analyzers and other instruments. A set of RVDs and current shunts has been designed for the power standard system. All the components are calibrated both in amplitude and phase angle errors. The uncertainty of ac power standard for 100 V and 100 A ranges from less than 35 $\mu\text{W}/\text{VA}$ at 400 Hz to 100 $\mu\text{W}/\text{VA}$ at 100 kHz at power factor 1.

REFERENCES

- [1] I. Budovsky, *Standard of electrical power at frequencies up to 200 kHz*, IEEE Transactions on Instrumentation and Measurement, vol. 58, no. 4, April 2009, pp. 1010–1016.
- [2] I. Budovsky, A. M. Gibbes, and D. C. Arthur, *A high-frequency thermal power comparator*, IEEE Transactions on Instrumentation and Measurement, vol. 48, no. 2, April 1999, pp. 427–430.
- [3] V. Tarasso, T. Bergsten, and K. E. Rydler, *Towards an electric power standard for frequencies up to 1 MHz*, Proc. Conf. Precis. Electromagn. Meas. Dig., Washington DC, July 1-6, 2012, pp. 128–129.
- [4] X. Pan, Z. Shi, et al., *Design and self-calibration of the RVD with serial-parallel connection*, Proc. Conf. Precis. Electromagn. Meas. Dig., Ottawa, July 10-15, 2016, pp. 1-2.
- [5] X. Pan, J. Zhang, et al., *A coaxial time constant standard for the determination of phase angle errors of current shunts*, IEEE Transactions on Instrumentation and Measurement, vol. 62, no. 1, January 2013, pp. 199–204.
- [6] X. Pan, J. Zhang, et al., *Measurement of the phase angle errors of high current shunts at frequencies up to 100 kHz*, IEEE Transactions on Instrumentation and Measurement, vol. 62, no. 6, June 2013, pp. 1652–1657.
- [7] G. Rietveld, D. Zhao, et al., *Characterization of a wideband digitizer for power measurements up to 1 MHz*, IEEE Transactions on Instrumentation and Measurement, vol.60, no.7, July 2011, pp.2195–2201.